

EFFECTS ON SOLAR RADIATIVE TRANSFER FOR STRATIFORM CLOUDS
DUE TO HORIZONTAL VARIATIONS IN CLOUD LIQUID WATER PATH
AND DROPLET EFFECTIVE RADIUS

Petri Räisänen *

Dalhousie University, Halifax, Nova Scotia, Canada

Howard W. Barker, George A. Isaac, and Ismail Gultepe

Cloud Physics Research Division, Meteorological Service of Canada, Downsview, Ontario, Canada

1. INTRODUCTION

The effects of cloud horizontal variability on solar radiative transfer have been studied extensively. Many of these studies have considered horizontally varying cloud water fields (e.g., from cloud resolving model simulations) in conjunction with constant droplet size distribution or effective radius r_e (e.g., Cahalan et al. 1994, Barker et al. 1999, Fu et al. 2000). Other studies have used optical thickness fields derived from satellite radiances, assuming a fixed r_e as well in the retrieval process as in radiative flux calculations (e.g., Barker 1996, Oreopoulos and Davies 1998). However, there appears to be no studies considering explicitly the horizontal variations in r_e . Yet aircraft observations indicate that r_e varies much in space and is often positively correlated with cloud liquid water content (LWC). The present work addresses the relative roles of variations in cloud water and r_e in stratiform liquid phase clouds using a Monte Carlo radiative transfer model and in-situ aircraft observations of cloud properties.

2. CLOUD DATA

The aircraft data used in this study were collected during the Radiation, Aerosol and Cloud Experiment (RACE) conducted over the Bay of Fundy and central Ontario in mid-August to early October 1995 (Gultepe et al., 2001). Eleven quasi-horizontal transects of LWC (from the Nevzorov hot wire probe) and r_e (from the forward scattering spectrometer probe (FSSP)) were selected for testing (Table 1). Three transects are from flights with the National Research Council of Canada Convair-580 (CON) aircraft, while eight are from Twin Otter (TW) flights. All transects are from stratiform water clouds with base heights below 1.5 km. In most cases both LWC and r_e increase with height in the cloud as typical of boundary layer clouds. The transects were collected at 1 sec temporal resolution, which corresponds to a horizontal resolution of ≈ 86 m for the Convair flights and ≈ 65 m for the Twin Otter flights.

The two most important assumptions employed to expand the one-dimensional transects of LWC and r_e into model clouds were that (1) the cloud bottom and top heights are constant (values estimated from aircraft data); and (2) that the cloud horizontal variations are perfectly correlated in the vertical and equally large at all levels in the cloud. That is, the ratios of LWC and r_e values at two heights z_1 and z_2 are independent of the horizontal location; e.g.,

$$\text{LWC}(x, y, z_2) / \text{LWC}(x, y, z_1) = f(z_1, z_2) \quad (1)$$

In the vertical, LWC and r_e are either assumed to be constant (in the TW_04B and TW_10 cases) or to roughly follow “adiabatic-like” profiles ($\text{LWC} \sim z$, $r_e \sim z^{1/3}$). Sensitivity tests indicated that the effects of cloud horizontal variations depend little on the assumed vertical profiles of LWC and r_e so far the liquid water path (LWP) and column-mean r_e are not affected. Finally, cloud properties are assumed not to vary in the direction perpendicular to the aircraft transect (i.e., the clouds are treated as two-dimensional).

Table 1 summarizes the length of transect (L), cloud fraction (N), estimated cloud thickness (Δz), and cloud mean LWP, r_e and optical thickness (τ) in the eleven cases. Selected measures of cloud variability are displayed in Table 2. σ_{LWP} , σ_{r_e} , and σ_{τ} are the relative standard deviations of LWP, r_e and τ , respectively, and R is the linear correlation coefficient between LWC and r_e . Finally, b is the exponent in the power-law fit

$$r_e = a \times \text{LWC}^b. \quad (2)$$

The dataset covers a substantial range of cloud properties both in terms of mean values and horizontal variability, although generally the horizontal variations are fairly modest (as typical of stratiform clouds). Note also that R ranges from near zero in the TW_24B case to over 0.7 in a few cases, and with one exception (CON_15) b is below the value 1/3 expected for clouds with constant droplet number concentration.

3. RADIATION CALCULATIONS

The radiation calculations were made with a three-dimensional broadband Monte Carlo code which includes cloud droplets, aerosols, gas absorption (by H_2O , O_3 , CO_2 , and O_2) and molecular scattering. The solar spectrum is divided into 25 intervals as in Freidenreich

* *Corresponding author address:* Petri Räisänen, Dept. of Physics and Atmospheric Science, Dalhousie University, Nova Scotia B3H 3J5, Canada. e-mail: praisane@atm.dal.ca.

and Ramaswamy (1999). Cloud water extinction coefficient is calculated as

$$\beta \cong \frac{3}{2} \frac{LWC}{\rho_w r_e}, \quad (3)$$

where ρ_w is the density of liquid water, while single-scattering albedo and scattering phase function are computed from Mie theory and tabulated as a function of r_e assuming an effective variance $v_e = 0.12$.

TABLE 1

FLIGHT	DATE	L	N	ΔZ	LWP	r_e	τ
CON_02	160895	82	0.94	180	26	12.3	3.2
TW_04B	210895	38	1.00	240	74	11.9	9.3
CON_06	300895	78	0.75	390	101	7.0	21.4
TW_10	300895	56	0.61	400	30	5.1	8.8
TW_11	300895	68	0.74	230	23	5.9	5.8
TW_13C	010995	45	1.00	240	54	6.7	12.2
TW_18A	080995	82	0.76	200	10	9.4	1.6
CON_15	090995	148	0.71	500	120	10.0	18.1
TW_19	090995	40	1.00	500	65	7.9	12.4
TW_21	090995	51	0.87	600	114	6.1	28.2
TW_24B	041095	93	0.92	250	66	6.0	16.4

Average cloud properties for the cases used in the radiative transfer tests. Read "160895" as 16 Aug 1995. Units: [L] = km, [ΔZ] = m, [LWP] = g m⁻², [r_e] = μ m. See text for the definitions.

TABLE 2

FLIGHT	σ_{LWP}	σ_{r_e}	σ_τ	R	b
CON_02	0.623	0.215	0.492	0.745	0.297
TW_04B	0.349	0.132	0.307	0.552	0.224
CON_06	0.561	0.098	0.525	0.499	0.096
TW_10	0.844	0.157	0.726	0.757	0.182
TW_11	0.493	0.146	0.482	0.247	0.060
TW_13C	0.297	0.136	0.255	0.527	0.251
TW_18A	0.602	0.172	0.518	0.587	0.185
CON_15	0.666	0.325	0.503	0.727	0.401
TW_19	0.416	0.084	0.356	0.778	0.164
TW_21	0.566	0.182	0.505	0.536	0.221
TW_24B	0.447	0.170	0.464	0.059	0.042

Measures of cloud variability. See text for the definitions.

The clouds were embedded into either midlatitude summer or subarctic summer (McClatchey et al., 1971) model atmospheres (the choice depending on the observed lower tropospheric temperatures) and the specific humidity in the cloud was assumed to equal the saturation value at the cloud temperature. Maritime aerosol (World Climate Programme 1983) with an optical thickness τ ($\lambda=550$ nm) = 0.1 was assumed to be well mixed between 0 and 2 km. A parameterization for sea surface bi-directional reflectance was used which typically resulted in a surface albedo of 0.06-0.07.

For each case, the total effect of cloud horizontal variability (ΔF_{tot}), the effect of cloud water horizontal variations (ΔF_{LWP}) and the effect of horizontal variations in r_e (ΔF_{r_e}) was estimated from the results of three runs:

$$\Delta F_{tot} = F_{ref} - F_{pph}, \quad (4)$$

$$\Delta F_{LWP} = F_{h_{r_e}} - F_{pph}, \quad (5)$$

$$\Delta F_{r_e} = F_{ref} - F_{h_{r_e}}. \quad (6)$$

Here, the subscript "ref" denotes a reference run which includes fully the variations in both LWC and r_e . The run "h_{r_e}" includes the variations in LWC but ignores horizontal variations in r_e (as typically in studies of cloud horizontal inhomogeneity). Finally, "pph" refers to the plane-parallel horizontally homogeneous approximation, which is generally used in large-scale models.

4. RESULTS

Table 3 displays diurnal mean results for the upward shortwave (SW) flux at the top of the atmosphere (TOA) (F_{TOA}^\uparrow). Insolation conditions for the latitude 45° N for 1 September are assumed in all cases, which yields a diurnal mean incoming SW flux of 373 Wm⁻² at the TOA.

TABLE 3

FLIGHT	ΔF_{tot}	ΔF_{LWP}	ΔF_{r_e}	ΔF (%)	$\Delta \sigma$ (%)
CON_02	-2.41	-4.35	1.94	-45	-21
TW_04B	-2.55	-3.54	0.99	-28	-12
CON_06	-7.85	-9.90	2.05	-21	-6
TW_10	-6.38	-9.68	3.30	-34	-14
TW_11	-3.78	-4.21	0.43	-10	-2
TW_13C	-1.68	-2.71	1.03	-38	-14
TW_18A	-0.96	-1.45	0.49	-34	-14
CON_15	-5.81	-10.76	4.95	-46	-24
TW_19	-3.43	-5.56	2.13	-38	-14
TW_21	-6.89	-9.14	2.25	-25	-11
TW_24B	-10.41	-10.12	-0.29	3	4

Diurnal mean results for the upward SW flux at the TOA. The units of ΔF_{tot} , ΔF_{LWP} , and ΔF_{r_e} are W m⁻².

Much as expected, the total effect of cloud horizontal inhomogeneity (ΔF_{tot}) is negative in all cases (i.e., cloud albedo is reduced), diurnal mean values being in the range -1 to -10 Wm⁻². The effect of horizontal variations in r_e varies a lot of from case to case, but with one exception (TW_24B) it is to counteract the effects of LWP variations, by up to 5 Wm⁻² in the CON_15 case. Consequently, the total effects of horizontal inhomogeneity ΔF_{tot} are smaller than the estimates obtained by considering only LWP variations (ΔF_{LWP}). The relative effect of horizontal variations in r_e , defined as $\Delta F(\%) = 100 \times (\Delta F_{tot} / \Delta F_{LWP} - 1)$, is substantial in many cases, exceeding 40% in the CON_02 and CON_15 cases. For comparison, Table 3 also shows the relative effect of r_e horizontal variations on the standard deviation of optical thickness ($\Delta \sigma(\%) = 100 \times (\Delta \sigma_\tau / \Delta \sigma_{LWP} - 1)$). Interestingly, $\Delta F(\%)$ is typically twice as large as $\Delta \sigma(\%)$. There are two main reasons for this. First, the effect of horizontal inhomogeneity on radiative fluxes (ΔF_{tot}) has a stronger than linear dependence on σ_τ . Second, variations in r_e cause horizontal variations not only in τ but also in other cloud optical parameters, scattering phase function being most significant for F_{TOA}^\uparrow .

The results for the net SW flux at the surface were similar to those for F_{TOA}^\uparrow . However, horizontal variations in r_e had little effect on cloud layer absorption, diurnal mean effects being below 0.1 Wm⁻² in all cases. The

effects on radiative heating rates were also generally small. There was a slight tendency for the horizontal variations in r_e to increase the heating in the upper parts of the clouds and to decrease it in the lower parts.

Finally, Fig. 1 displays ΔF_{tot} , ΔF_{LWP} and ΔF_{r_e} for the upward SW flux at the TOA as a function of the solar zenith angle θ_0 in three cases. In the CON_02 and CON_15 cases, which both feature a strong correlation between LWC and r_e , the horizontal variations in r_e offset at least 40% of the effect of cloud water variations at all θ_0 values. In the CON_02 case, which is rather thin optically (mean $\tau = 3.2$), ΔF_{r_e} reaches its absolute maximum at $\theta_0 = 45\text{--}60^\circ$, whereas in the thicker CON_15 case (mean $\tau = 18.1$) ΔF_{r_e} is largest ($\approx 20 \text{ W m}^{-2}$) when the sun is in the zenith. In the TW_24B case, in which LWC and r_e are almost uncorrelated, horizontal variations in r_e have rather little effect irrespective of θ_0 (they

even slightly reinforce the effect of LWP variations for small θ_0).

5. DISCUSSION

The above results are reasonable and qualitatively robust. Quantitatively, however, the calculations include significant uncertainty factors, particularly as regards the assumptions about the structure of clouds.

The assumption of constant cloud geometrical thickness is obviously an idealization. In reality, LWP variations result from horizontal variations in both LWC and cloud thickness, whereas only the former factor is included in our calculations. Consequently, the calculations could underestimate the variations in LWP and thereby overestimate the relative role of horizontal variations in r_e . Preliminary idealized radiative transfer tests confirm this point but do not suggest that thickness variations typical of stratiform clouds would reduce the role of r_e variations drastically.

The assumption that horizontal variations in LWC and r_e are perfectly correlated in the vertical and equally large at all levels in the cloud is also an idealization. The effects of this assumption are difficult to quantify. On average, it probably leads to some overestimation of the variability of LWP and column-mean r_e , but this overestimation might not be severe for the relatively thin clouds considered here.

Finally, the aircraft measurements of LWC and r_e are not exact. The possibly most relevant point for the present study is that these measurements are from different instruments, so random errors in the two quantities are likely uncorrelated. This may decrease the measured correlation between LWC and r_e , which would tend to lead to a slight underestimation of the effects of horizontal variability in r_e . An additional set of calculations in which both LWC and r_e were inferred from FSSP data yielded tentative support for this idea: the effects of r_e variations on F_{TOA}^\uparrow were typically $\sim 20\%$ larger than those in Table 1.

6. CONCLUSIONS

The dominant impact of cloud horizontal inhomogeneity comes from cloud water variability, which reduces the cloud radiative effects compared to a corresponding horizontally homogeneous cloud. The effects of horizontal variations in r_e , which have been ignored in previous studies, vary a lot from case to case. In some cases they offset a substantial part of the effect of cloud water variations on the TOA and surface shortwave fluxes. The present study concerns only stratiform boundary layer water clouds with fairly modest horizontal variability. However, the effects of horizontal variations in cloud droplet (or ice crystal) size are likely worth considering also for other cloud types.

Acknowledgments. This work has been performed as part of the Modeling of Clouds and Climate (MOC2) project being funded by the Canadian Foundation for Climate and Atmospheric Sciences, the Natural Sci-

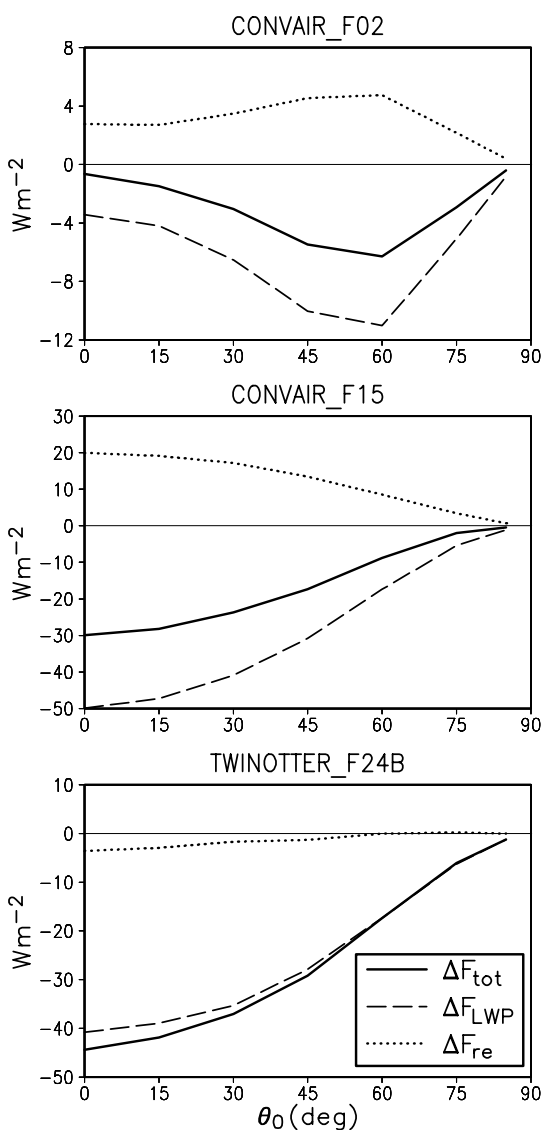


Figure 1. Results for the upward SW flux at the TOA as a function of the cosine of the solar zenith angle θ_0 in three cases.

ences and Engineering Research Council of Canada, and the Meteorological Service of Canada.

REFERENCES

- Barker, H. W., 1996: Estimating cloud field albedo using one-dimensional series of optical depth. *J. Atmos. Sci.*, **53**, 2826-2837.
- Barker, H. W., G. L. Stephens, and Q. Fu, 1999: The sensitivity of domain-averaged solar fluxes to assumptions about cloud geometry. *Quart. J. Roy. Meteor. Soc.*, **125**, 2127-2152.
- Cahalan, R. F., W. Ridgway, W. J. Wiscombe, T. L. Bell, and B. Snider, 1994: The albedo of fractal stratocumulus clouds. *J. Atmos. Sci.*, **51**, 2434-2455.
- Fu, Q., M. C. Cribb, H. W. Barker, S. K. Krueger and A. Grossman, 2000: Cloud geometry effects on atmospheric solar absorption. *J. Atmos. Sci.*, **57**, 1156-1168.
- Gultepe, I., G. A. Isaac, and K. B. Strawbridge, 2001: Variability of cloud microphysical and optical parameters obtained from aircraft and satellite remote sensing measurements during RACE. *Int. J. Climatol.*, **21**, 507-525.
- Freidenreich, S. M., and V. Ramaswamy, 1999: A new multiple-band solar radiative parameterization for general circulation models. *J. Geophys. Res.*, **104**, 31389-31409.
- McClatchey, R. A., R. W. Fenn, J. E. A. Selby, F. E. Volz, and J. S. Garing, 1971: Optical properties of the atmosphere. Rep. AFCRL-71-0279, 85 pp. [Available from Air Force Geophysics Laboratory, Hanscom Air Force Base, MA 01731.]
- Oreopoulos, L., and R. Davies, 1998: Plane parallel albedo biases from satellite observations. Part I: Dependence on resolution and other factors. *J. Climate*, **11**, 919-932.
- World Climate Programme, 1983: Report of the experts meeting on aerosols and their climatic effects, Williamsburg, Virginia, 28-30 March 1983. Rep. WCP-55, WMO-CAS and IAMAP Radiation Commission, WMO, Geneva, Switzerland.